Available online at www.sciencedirect.com

SciVerse ScienceDirect

Ceramics International 39 (2013) 3261–3268

CERAMICS INTERNATIONAL

www.elsevier.com/locate/ceramint

Effect of film thickness and annealing temperature on the structural and optical properties of ZnO thin films deposited on sapphire (0001) substrates by sol–gel

Lin Cui[a,*], Gui-Gen Wang[a,*], Hua-Yu Zhang[a], Rui Sun[a], Xu-Ping Kuang[a], Jie-Cai Han[a,b]

[a]*Shenzhen Graduate School, Harbin Institute of Technology, Shenzhen 518055, PR China*
[b]*Center for Composite Materials, Harbin Institute of Technology, Harbin 150080, PR China*

Received 13 July 2012; received in revised form 3 October 2012; accepted 4 October 2012
Available online 23 October 2012

Abstract

ZnO thin films were prepared on sapphire (0001) substrates by the dip-coating sol–gel technique. Then, ZnO thin films with thicknesses of 50 nm, 150 nm, 250 nm, and 350 nm were annealed at 800 °C and with thickness of 250 nm were annealed at 600 °C, 700 °C, 800 °C, and 900 °C, respectively. The effect of film thickness and annealing temperature on the structure and optical properties of sol–gel ZnO thin films on sapphire substrates were investigated by XRD, SEM, RT-PL. All the sol–gel ZnO thin films show polycrystalline hexagonal wurtzite structure and a high preferential *c*-axis orientation. The XRD and SEM results show that the better structural quality, high *c*-axis preferred orientation, uniform, compact sol–gel ZnO thin films 250 nm thick were obtained when annealed at 700 °C in air. Room-temperature PL spectrum of sol–gel ZnO thin films can be divided into the UV emission and the visible broad band emission. The UV emission can be attributed to the near band edge emission (NBE) and the visible broadband emission can be ascribed to the deep level emissions (DLE). The visible emission is suppressed with the annealing temperature of 600–700 °C. By analyzing our experimental results, we concluded that the deep-level emission corresponds to oxygen vacancies (V_O). The biggest ratio of the PL intensity of UV emission to that of visible emission (I_{NBE}/I_{DLE}) is observed from sol–gel ZnO thin films 250 nm thick annealed at 700 °C. Therefore, we suggest that film thickness of 250 nm and annealing temperature of 700 °C are the most suitable conditions for obtaining high quality, high c-axis preferred orientation, uniform, compact sol–gel ZnO thin films with good luminescence performance.

Keywords: ZnO; Sol–gel; Annealing; X-ray diffraction

1. Introduction

ZnO has been of great interest recently due to its direct and wide band gap of 3.36 eV and a relatively higher exciton binding energy of 60 meV at room temperature [1]. In addition, ZnO possesses many excellent and unique properties for applications in optoelectronic such as light emitting diodes (LEDs) [2], acoustic devices [3], gases sensors [4], photodetectors [5], and solar cells [6], etc. A number of techniques have been used for fabrication of ZnO thin films, including chemical vapor deposition (CVD) [7], magnetron sputtering [8], molecular beam epitaxy (MBE) [9], spray-pyrolysis [10], pulsed laser deposition (PLD) [11], sol–gel [12].

In recent years, there has been an increasing interest in the growth of ZnO thin films by sol–gel [13–18]. This is due to the advantages of sol–gel technology in terms of being simple, accurate in doping control, suitable for large-scale production, low-cost, and low in energy consumption to investigate structure and optical properties of ZnO thin films. In this study, ZnO thin films were deposited on sapphire (0001) substrates by the dip-coating sol–gel method. The effect of film thickness and annealing temperature on the structure and optical properties of sol–gel ZnO thin films on sapphire (0001) substrates were investigated by X-ray diffraction (XRD), scanning electron microscope (SEM), photoluminescence (PL).

*Corresponding authors.
E-mail addresses: cuilin0512@gmail.com (L. Cui), wanggghit@163.com (G.-G. Wang).

0272-8842/$ - see front matter
http://dx.doi.org/10.1016/j.ceramint.2012.10.014

2. Experimental

ZnO thin films were prepared on sapphire (0001) substrates by the dip-coating sol–gel technique. Fig. 1 shows the flow chart of sol–gel process and dip coating technique in producing ZnO thin films. Zinc acetate dihydrate ($Zn(CH_3COO)_2 \cdot 2H_2O$), 2-methoxyethanol ($CH_3OCH_2CH_2OH$) and monoethanolamine ($HOCH_2CH_2NH_2$) were used as starting material, solvent and stabilizer, respectively. There are several major steps in this experiment which are the preparation of the solution and substrate, deposition process, pre-heating, annealing and characterization process. The molar ratio of MEA to zinc acetate dehydrate was maintained at 1:1 and the concentration of zinc acetate was 0.75 mol. The sapphire (0001) substrates were ultrasonically cleaned in acetone for 10 min, alcohol for 10 min, rinsed in deionized water, and then dried in N_2. The resulting mixture was stirred for 3 h at 65 °C to yield a clear and homogeneous solution, which was served as coating solution after cooling to room temperature. The dip coating was usually made 24 h after the solution was prepared. ZnO thin films were fabricated by dipping the sapphire substrates into the coating solution with withdrawal speeds of 18 mm/min at room temperature. After the coating process, the thin films are dried at 300 °C immediately for 10 min in a furnace. The film was then inserted into a tube furnace and annealed in air. It is also sometimes known as post-heating treatment.

In order to investigate the effect of film thickness and annealing temperature, first, after the dip coating process, the thin films are dried at 300 °C immediately for 10 min in a furnace, which was repeated for 1, 3, 5 and 7 times in order to get ZnO thin films with different thicknesses; correspondingly, the thickness of ZnO thin films was about 50, 150, 250 and 350 nm, respectively. Then, the coated films were annealed for 2 h at 800 °C in a furnace. Second, after the dip coating process, the thin films are dried at 300 °C immediately for 10 min in an air furnace. This process was repeated for 5 times. Then, the coated films were annealed for 2 h at 600, 700, 800, and 900 °C in an air furnace.

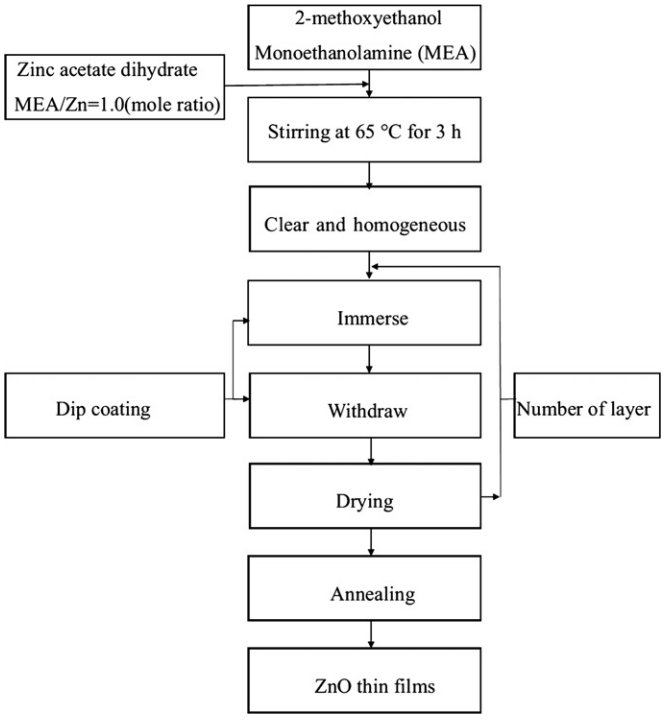

Fig. 1. Flow chart of sol–gel process and dip coating technique in producing ZnO thin films.

The microstructure and stresses in ZnO thin films were investigated by X-ray diffraction (XRD: Ricoh Company D/max 2500PC) using Cu Ka radiation ($\lambda = 0.15406$ nm). The surface morphology and thickness of ZnO thin films were examined by scanning electron microscope (SEM: HITACHI S-4700). The optical properties and crystal defects were examined by room-temperature photoluminescence (RT-PL: Renishaw Invia Reflex) using a He–Cd laser ($\lambda = 325$ nm) as the excitation source.

3. Results and discussion

The XRD patterns of the sol–gel ZnO thin films with different thicknesses annealed at 800 °C and with thickness of 250 nm annealed at various temperatures are shown in Fig. 2(a) and Fig. 2(b), respectively. The measured XRD pattern in Fig. 2 demonstrates that all the sol–gel grown ZnO thin films show seven relatively higher sharp and narrow diffraction peaks, which are identified to be originated from (100), (002), (101), (102), (110), (103) and (112) reflections of hexagonal ZnO crystal (PDF 36–1451). The XRD results indicate that all the ZnO thin films are polycrystalline hexagonal wurtzite structure. The sample is polycrystalline but the intensity of the (002) peak at $2\theta = 34.45^\circ$ larger than those of the other peaks indicates that the sol–gel ZnO films are preferentially oriented with the c-axis perpendicular to the film surface. It was also observed that, by increasing the film thickness and annealing temperature, an enhancement of the intensity for all diffraction peaks occurs in general. However, a sharp increase for the (002) plane is observed compared to others. The smaller FWHM and stronger diffraction intensity mean the better crystal quality of sol–gel ZnO thin films. Fig. 3(a) shows that the diffraction intensity and FWHM of diffraction peak (002) in sol–gel ZnO thin films as a function of film thickness. The diffraction intensity obviously increases with the film thickness and reaches to the maximum at 250 nm, after that it decreased at 350 nm. As the film thickness increases up to 350 nm, the FWHM reach to the minimum of 0.283° at 250 nm and then increase.

It was also reported that the preferential crystal orientation of ZnO thin films has a profound impact on ZnO-based device properties [19]. Therefore, in order to precisely investigate the effect of film thickness and annealing temperature on the degree of orientation of the (002) plane

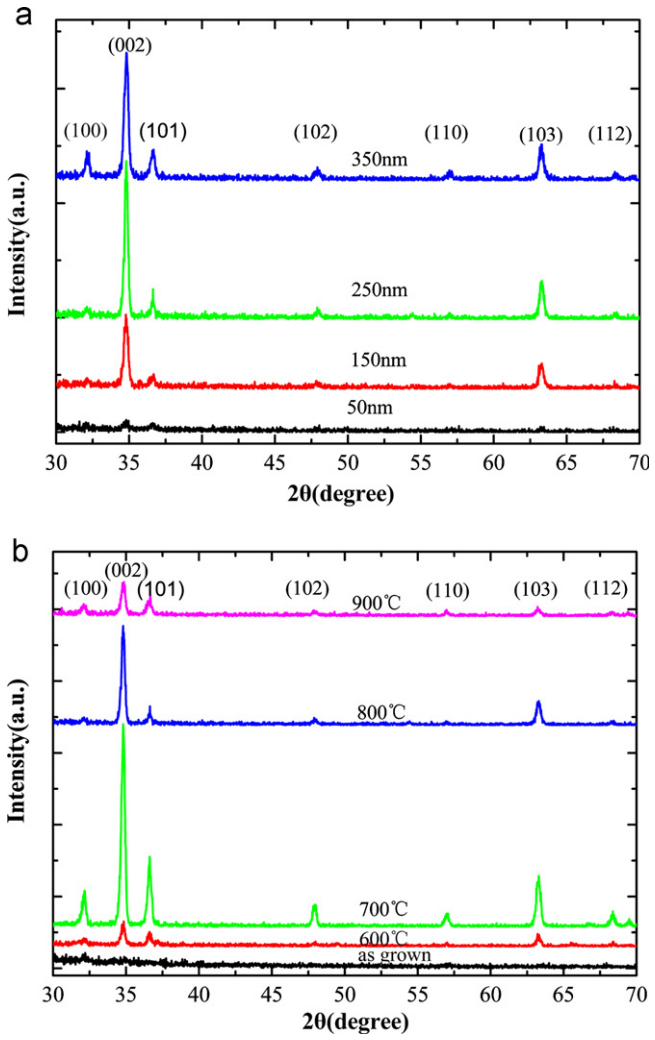

Fig. 2. XRD patterns of the sol–gel ZnO thin films with different thicknesses annealed at 800 °C (a) and with thickness of 250 nm annealed at various temperatures (b).

a formula proposed by Lotgering was used [20]:

$$F(\mathrm{hkl}) = \frac{P(\mathrm{hkl}) - P_0(\mathrm{hkl})}{1 - P_0(\mathrm{hkl})} \quad (1)$$

where F(hkl) is the degree of (hkl) orientation, $P(\mathrm{hkl}) = I(\mathrm{hkl})/\sum I(\mathrm{hkl})$ and $P_0(\mathrm{hkl}) = I_0(\mathrm{hkl})/\sum I_0(\mathrm{hkl})$. Here I(hkl) is the (hkl) peak intensity and $\sum I$(hkl) is the sum of the intensities of all peaks in the ZnO thin films' diffraction data. I_0(hkl) is the (hkl) peak intensity and $\sum I_0$(hkl) is the sum of the intensities of diffraction peaks in the reference data (JCPDS 36–1451). Fig. 3(c) shows that the values of degree of orientation of the (002) plane in sol–gel ZnO thin films as a function of film thickness. As the film thickness is increased, (002) orientation is preferred and becomes maximum for the thickness of 250 nm. Above this thickness, the film again becomes randomly oriented. Poor crystallinity in thinner ZnO thin films could be associated with an incomplete growth of the crystallites as only few atomic layers of disordered atoms constitute the bulk of the film [21]. According to the mechanism of crystal growth [22,23], the growing faces of crystallites correspond to the crystal shape at equilibrium and are determined by the orientation of the crystal. A growth competition can start among the neighboring crystals according to their growth types (i.e., to their orientation). The faster growing crystals will grow over the slower growing ones. This competition is terminated when only crystals exhibiting the same type of crystal faces proceed to form the free surface. This competitive crystal growth represents an orientation selection resulting in the competitive growth texture [24]. This was probably why the crystallinity was increased when ZnO thin films were thicker. The XRD results revealed that the better crystallinity and highly preferential orientation of (002) plane of sol–gel ZnO thin films were obtained with thickness of 250 nm.

The SEM surface morphology for the ZnO thin films annealed at 800 °C with different thicknesses varying from 50 to 350 nm are shown in Fig. 4. It is observed that the grain size increases and packing density increases when the film thickness increases. When the film thickness is in the range 50–150 nm, the grains become non-uniform in size and ZnO thin films become loose. The grains become more uniform and bigger in size and ZnO thin films become denser as the film thickness increases up to 250 nm. The inset shows the cross-sectional SEM image of sol–gel ZnO thin films 250 nm thick (Fig. 4(c)). ZnO thin films become again loose as the film thickness increases up to 350 nm. The XRD and SEM results show that the optimum thickness of compact sol–gel ZnO thin films with the best structural quality and high c-axis preferred orientation could be up to around 250 nm.

The diffraction intensity and FWHM of diffraction peak (002) in sol–gel ZnO thin films as a function of annealing temperature are shown Fig. 3(b). The diffraction intensity obviously increases with the annealing temperature of 600–700 °C and reaches to the maximum at 700 °C, after that it decreased with the annealing temperature of 700–900 °C. The FWHM obviously decreases with the annealing temperature of 600–700 °C and reaches to the minimum at 700 °C, after that it increased with the annealing temperature of 700–900 °C. Fig. 3(d) shows the values of degree of orientation of the (002) plane of sol–gel ZnO thin films as a function of annealing temperature. The values of degree of orientation of the (002) plane increases with the annealing temperature of 600–700 °C and reaches to the maximum at 700 °C, after that it decreased with the annealing temperature of 700–900 °C. This result can be explained by the two reasons: At first, annealing increases atomic mobility, enhancing the ability of atoms to find the most energetically favored sites. At second, with the increase of the annealing temperature, the densities of the crystallographic defects including dislocations, interstitials and vacancies in sol–gel ZnO thin films decrease rapidly. These two reasons can lead to yield the best structural property of sol–gel ZnO thin films 250 nm thick annealed at 700 °C. A further increase in the temperature up to

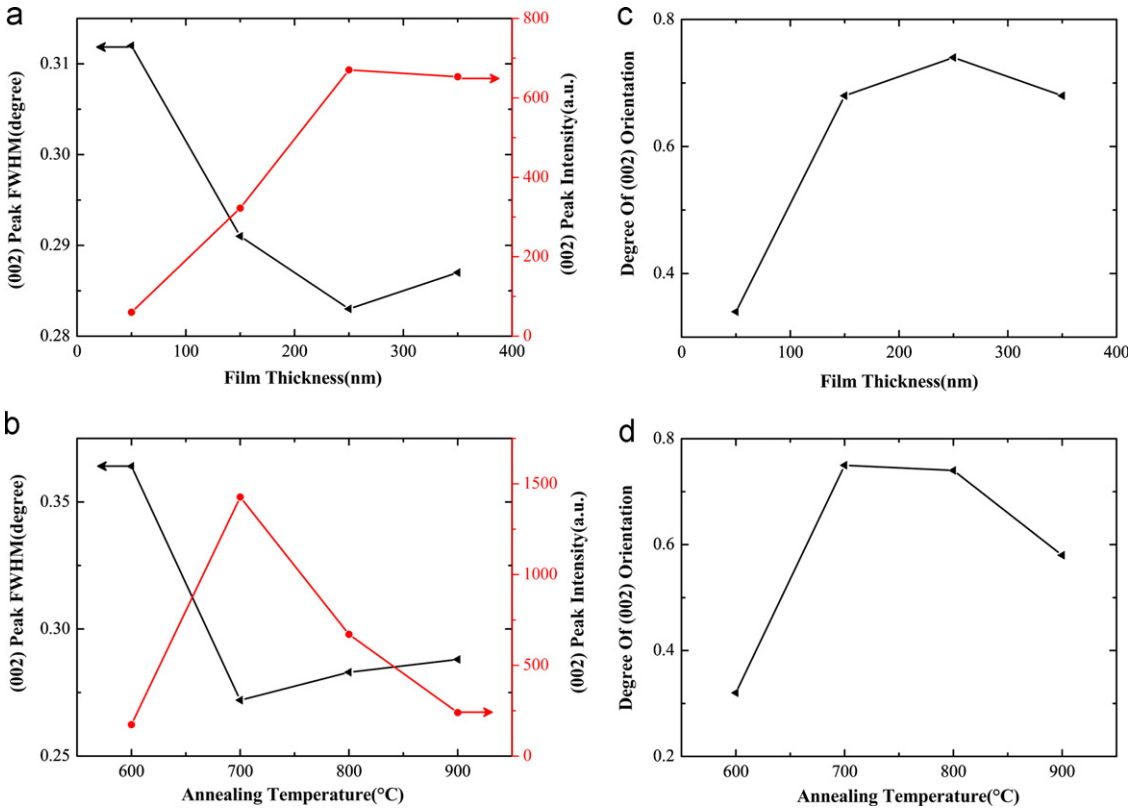

Fig. 3. Diffraction intensity and FWHM of diffraction peak (0 0 2) as a function of sol–gel ZnO thin films with different thicknesses annealed at 800 °C (a) and with thickness of 250 nm annealed at various temperatures (b), and the values of degree of orientation of the (002) plane as a function of sol–gel ZnO thin films with different thicknesses annealed at 800 °C (c) and with thickness of 250 nm annealed at various temperatures (d).

900 °C leads to the decrease of crystal quality because sol–gel ZnO thin films is thermodynamically unstable with in a rich-oxygen atmosphere leading to its evaporative dissociation into Zn and O_2 [25]. In the reported reference [26], the FWHM value is 0.25° of MOVPE grown ZnO on an r-plane sapphire substrate. In our experiment, the FWHM value is 0.272° of sol–gel grown ZnO thin films 250 nm thick at the annealing temperature of 700 °C in air, revealing that the high quality and highly preferential orientation of (002) plane of sol–gel ZnO thin films could be also obtained by optimized film thickness and high temperature annealing treatment.

The SEM surface morphology for the sol–gel ZnO thin films 250 nm thick annealed at different temperatures are shown in Fig. 5. It is observed that the grain size increases and packing density increases when the annealing temperature increases. When the annealing temperature is 600 °C, the grains become non-uniform in size and sol–gel ZnO thin films become loose. The grains become more uniform in size and sol–gel ZnO thin films become denser as the annealing temperature is in the range 700–800 °C. As the annealing temperature increases up to 900 °C, the voids were found on the loose surface of sol–gel ZnO thin films. The XRD and SEM results show that the optimum film thickness and annealing temperature of compact sol–gel ZnO thin films with the best structural quality and high c-axis preferred orientation could be up to around 250 nm and 700 °C, respectively.

Room-temperature PL spectra of sol–gel ZnO thin films with various thicknesses annealed for 2 h at 800 °C in air are shown in Fig. 6(a). As shown in the figure, the spectrum can be divided into the UV (~380 nm) and the visible light (500–700 nm) parts. The UV emission can be attributed to the near band edge emission (NBE) and originate from the recombination of free excitons. It is well known that the visible emission of ZnO thin films is due to defects that form deep energy levels in the band gap [27,28]. Generally, a common method for evaluating the concentration of structural defects in ZnO thin films is based on the ratio of the PL intensity of UV light emission to that of visible light emission (I_{NBE}/I_{DLE}) [29]. Fig. 7(a) demonstrates the PL intensity ratio and UV emission intensity of sol–gel ZnO thin films with various thicknesses annealed at 800 °C in air. The UV emission obviously increases with the film thickness increasing and reaches to the maximum at 250 nm, after that it decreased at 350 nm. The PL ratio increased from the film thickness of 50–250 nm and decreased at 350 nm. The bigger the ratio R, the higher the quality of the ZnO thin films [30]. This result revealed that less defects were generated when the thickness of sol–gel ZnO thin films was 250 nm. It is consistent with the results of XRD.

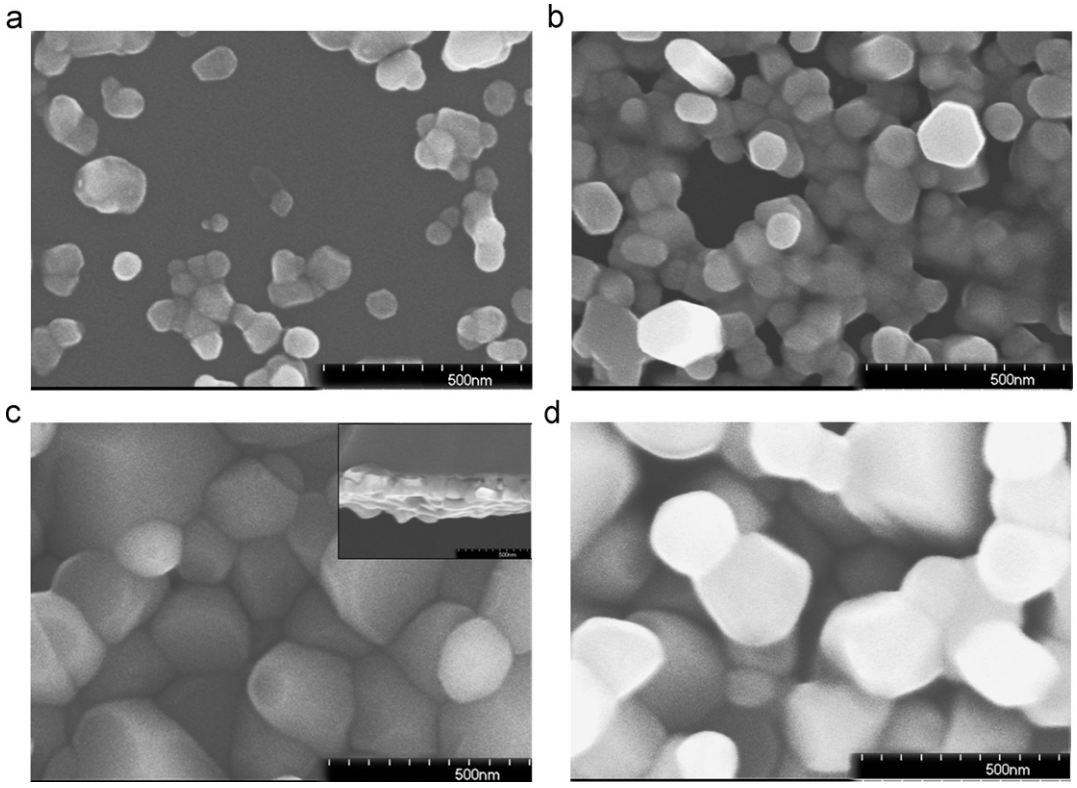

Fig. 4. SEM surface images of sol–gel ZnO thin films annealed at 800 °C with different thicknesses: 50 nm (a), 150 nm (b), 250 nm (c), and 350 nm (d), respectively.

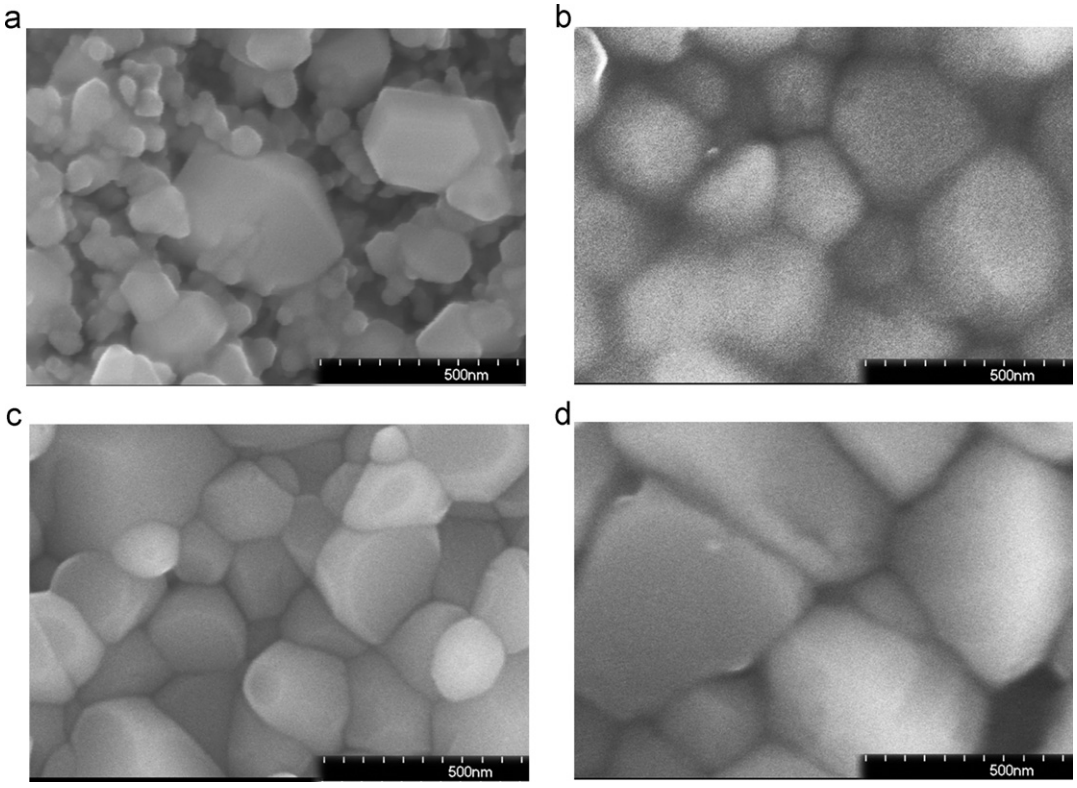

Fig. 5. SEM surface images of sol–gel ZnO thin films 250 nm thick annealed at various temperatures: 600 °C (a), 700 °C (b), 800 °C (c), and 900 °C (d), respectively.

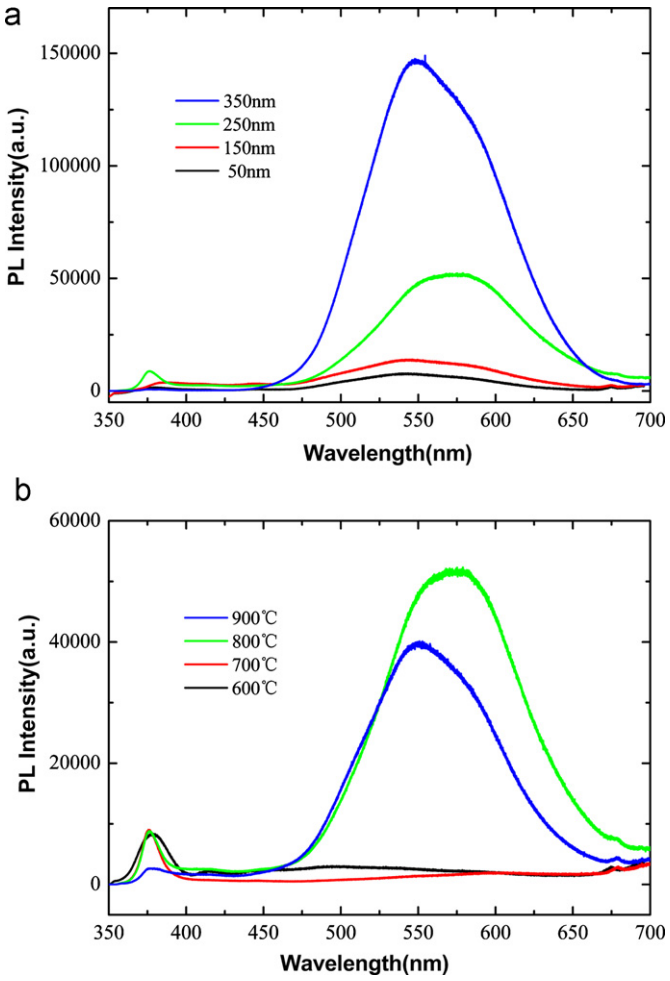

Fig. 6. Room-temperature PL spectra of the sol–gel ZnO thin films with different thicknesses annealed at 800 °C (a) and with thickness of 250 nm annealed at various temperatures (b).

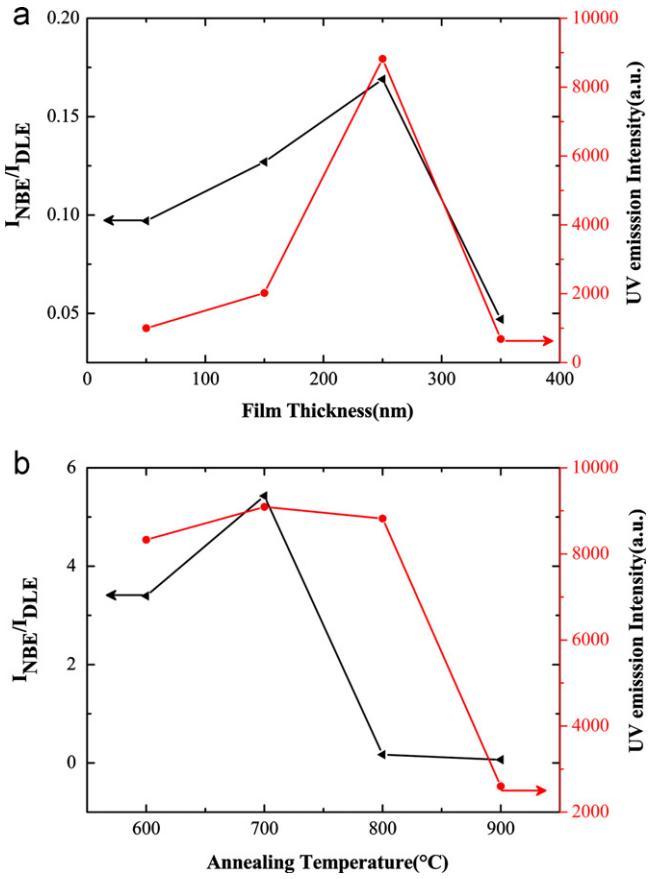

Fig. 7. I_{NBE}/I_{DLE} and UV emission intensity as a function of sol–gel ZnO thin films with different thicknesses annealed at 800 °C (a) and with thickness of 250 nm annealed at various temperatures (b).

Room-temperature PL spectra of sol–gel ZnO thin films 250 nm thick annealed for 2 h in air at various temperatures are shown in Fig. 6(b). As shown in the figure, the spectrum can be divided into the UV (~380 nm) and the visible light (500–700 nm) parts. Fig. 7(b) demonstrates the UV emission intensity of sol–gel ZnO thin films 250 nm thick annealed for 2 h in air at various temperatures. The UV emission obviously increases with the annealing temperature of 600–700 °C and reaches to the maximum at 700 °C, after that it decreased with the annealing temperature of 700–900 °C. Moreover, as shown in the Fig. 6(b), the visible emission is suppressed with the annealing temperature of 600–700 °C indicating better quality of sol–gel ZnO thin films. However, the visible emission is rapid increased with the annealing temperature of 700–900 °C. The luminescence center is the strong and broad green emission at 550 nm resulted primarily from oxygen vacancies [31,32]. Past research had found that increased of oxygen vacancies (V_O) will result in the increased of visible luminescence because when annealed in air at higher temperature, sol–gel ZnO thin films tend to lose the oxygen [33]. From this investigation, it could be considered that increase of oxygen vacancies (V_O) is the cause of rapid increased in visible emission as the annealing temperature of 700–900 °C. Fig. 7(b) demonstrates the PL intensity ratio of sol–gel ZnO thin films 250 nm thick annealed for 2 h in air at various temperatures. The PL intensity ratio increases with the annealing temperature of 600–700 °C and reaches to the maximum at 700 °C, after that it decreased with the annealing temperature of 700–900 °C. This result revealed that less defects were generated when ZnO thin films were annealed at 700 °C in air. It is evident that sol–gel ZnO thin films 250 nm thick annealed for 2 h in air at 700 °C exhibit the largest improvement in the luminescent efficiency.

4. Conclusion

ZnO thin films were prepared on sapphire (0001) substrates by the dip-coating sol–gel technique. Then, ZnO thin films with thicknesses of 50 nm, 150 nm, 250 nm, and 350 nm were annealed at 800 °C and with thickness of 250 nm were annealed at 600 °C, 700 °C, 800 °C, and 900 °C, respectively. The effect of film thickness and annealing temperature on the structure and optical properties of sol–gel ZnO thin films on sapphire

(0001) substrates were investigated by XRD, SEM, RT-PL. All the sol–gel ZnO thin films show polycrystalline hexagonal wurtzite structure and a high preferential c-axis orientation. The XRD and SEM results show that the better structural quality, high c-axis preferred orientation, uniform, compact sol–gel ZnO thin films 250 nm thick were obtained when annealed at 700 °C in air. Room-temperature PL spectrum of sol–gel ZnO thin films can be divided into the UV emission and the visible broad band emission. The UV emission can be attributed to the near band edge emission (NBE) and the visible broad band emission can be ascribed to the deep level emissions (DLE). The visible emission is suppressed with the annealing temperature of 600–700 °C. By analyzing our experimental results, we assumed that the deep-level emission corresponds to oxygen vacancies (V_O). The sol–gel ZnO thin films 250 nm thick annealed for 2 h in air at 700 °C exhibit the largest improvement in the luminescent efficiency. Therefore, we suggest that film thickness of 250 nm and annealing temperature of 700 °C are the most suitable conditions for obtaining high quality, high c-axis preferred orientation, uniform, compact sol–gel ZnO thin films with good luminescence performance.

Acknowledgments

This project was supported by the National Natural Science Foundation of China (Grant nos. 50902028 and 51172054), International Science and Technology Cooperation Program of Sino-Russian (Grant no. 2009DFR50350), the Natural Science Foundation of Guangdong Province (Grant no. 9451805707003351), the Basic Research Plan Program of Shenzhen City (Grant no. JC200903120169A) and the Natural Scientific Research Innovation Foundation in Harbin Institute of Technology (Grant no. HIT.NSFIR.2011123).

References

[1] Y. Gu, I.L. Kuskovsky, M. Yin, S. O'Brien, G.F. Neumark, Quantum confinement in ZnO nanorods, Applied Physics Letters 85 (2004) 3833.
[2] T. Soki, Y. Hatanaka, D.C. Look, ZnO diode fabricated by excimer-laser doping, Applied Physics Letters 76 (2000) 3257.
[3] T. Mitsuyu, S. Ono, K. Wasa, Structures and SAW properties of RF-sputtered single-crystal films of ZnO on sapphire, Journal of Applied Physiology 51 (1980) 2646.
[4] Camelia Matei Ghimbeu, Joop Schoonman, Martine Lumbreras, Maryam Siadat, Electrostatic spray deposited zinc oxide films for gas sensor applications, Applied Surface Science 253 (2007) 7483–7489.
[5] X.Q. Tan, Z.Q. Wu, W. Zhi, Photovoltaic behavior and work function of zinc oxides as solar cells, Applied Surface Science 257 (2010) 1141–1144.
[6] Han Gil Na, Ju Chan Yang, Dong Sub Kwak, Hyoun Woo Kim, Bismuth-catalyzed synthesis of ZnO nanowires and their photoluminescence properties, Ceramics International 38 (2012) 3659–3666.
[7] Guangyao Zhu, Shulin Gu, Shunming Zhu, Shimin Huang, Ran Gu, Jiandong Ye, Youdou Zheng, Optimization study of metal-organic chemical vapor deposition of ZnO on sapphire substrate, Journal of Crystal Growth 349 (2012) 6–11.
[8] Lin Cui, Hua-Yu Zhang, Gui-Gen Wang, Fang-Xu Yang, Xu-Ping Kuang, Rui Sun, Jie-Cai Han, Effect of annealing temperature and annealing atmosphere on the structure and optical properties of ZnO thin films on sapphire (0001) substrates by magnetron sputtering, Applied Surface Science 258 (2012) 2479–2485.
[9] J.H. Liang, H.Y. Lai, Y. Chen, Morphology transition of ZnO films with DMZn flow rate in MOCVD process, Applied Surface Science 256 (2010) 7305–7310.
[10] P. Fons, K. Iwata, S. Niki, A. Yamada, K. Matsubara, Growth of high-quality epitaxial ZnO films on α-Al_2O_3, Journal of Crystal Growth 201 (1999) 627-623.
[11] Xu Linhua, Li Xiangyin, Chen Yulin, Fei Xu, Structural and optical properties of ZnO thin films prepared by sol–gel method with different thickness, Applied Surface Science 257 (2011) 4031–4037.
[12] D.H. Bao, H.S. Gu, A. Kuang, Sol–gel-derived c-axis oriented ZnO thin films, Thin Solid Films 312 (1998) 37–39.
[13] M.N. Kamalasanan, S. Chandra, Sol–gel synthesis of ZnO thin films, Thin Solid Films 288 (1996) 112–115.
[14] J.H. Lee, K.H. Ko, B.O. Park, Electrical and optical properties of ZnO transparent conducting films by the sol-gel method, Journal of crystal growth 247 (2003) 119–125.
[15] Linhua Xu, Gaige Zheng, Juhong Miao, Fenglin Xian, Dependence of structural and optical properties of sol-gel derived ZnO thin films on sol concentration, Applied Surface Science 258 (2012) 7760–7765.
[16] Seung Hwangbo, Yun-Ji Lee, Kyu-Seog Hwang, Photoluminescence of ZnO layer on commercial glass substrate prepared by sol-gel process, Ceramics International 34 (2008) 1237–1239.
[17]β Kyu-Seog Hwang, Bo-An Kang, Yu-Sang Kim, Seung Hwangbo, Jin-Tae Kim, Heteroepitaxial ZnO/sapphire (0001) structure prepared by sol–gel process, Ceramics International 36 (2010) 2259–2262.
[18] Nanda Shakti, P.S. Gupta, Structural and optical properties of sol–gel prepared ZnO thin film, Applied Physics Research 2 (2010) 19–28.
[19] B.S. Ong, C. Li, Y. Li, Y. Wu, R. Loutfy, Stable, solution-processed, high-mobility ZnO thin-film transistors, Journal of the American Chemical Society 129 (2007) 2750–2751.
[20] F.K. Lotgering, Topotactical reactions with ferromagnetic oxides having hexagonal crystal structures-I, Journal of Inorganic and Nuclear Chemistry 9 (1959) 113–123.
[21] J.Y.W. Seto, The electrical properties of polycrystalline silicon films, Journal of Applied Physics 46 (1975) 5247.
[22] A. Van Der Drift, Evolutionary selection, A principle governing growth orientation in vapor-deposited layers, Philips Research Reports 22 (1967) 267–288.
[23] G. Knuyt, C. Quaeyhaegens, J.D. Haen, L.M. Stals, A model for thin film texture evolution driven by surface energy effects, Physica Status Solidi B 195 (1996) 179–182.
[24] P.B. Barna, M. Adamik, Fundamental structure forming phenomena of polycrystalline films and the structure zone models, Thin Solid Films 317 (1998) 27–33.
[25] Shulin Gu, Rong Zhang, Jingxi Sun, Ling Zhang, T.F. Kuech, Role of interfacial compound formation associated with the use of ZnO buffers layers in the hydride vapor phase epitaxy of GaN, Applied Physics Letters 76 (2000) 3454–3456.
[26] V. Gupta, A. Mansingh, Influence of postdeposition annealing on the structural and optical properties of sputtered zinc oxide film, Journal of Applied Physics 80 (1996) 1063–1073.
[27] K. Vanheusden, W.L. Warren, C.H. Seager, D.R. Tal-lant, J.A. Voigt, B.E. Gnade, Mechanisms behind green photoluminescence in ZnO phosphor powders, Journal of Applied Physics 79 (1996) 7983–7990.
[28] D.K. Lee, S. Kim, M.C. Kim, S.H. Eom, H.T. Oh, S.H. Choi, Annealing effect on the electrical and the optical characteristics of undoped ZnO thin films grown on Si substrates by RF magnetron sputtering, Journal of Korean Physical Society 51 (2007) 1378–1382.
[29] P.T. Hsieh, Y.C. Chen, K.S. Kao, C.M. Wang, Transparence and electrical properties of non-stoichiometric ZnO films by various

sputtering and annealing temperatures, Physica B 403 (2008) 178–183.
[30] L. Martinu, D. Poitras, Plasma deposition of optical films and coatings: a review, Journal of Vacuum Science and Technology A 18 (2000) 2619–2645.
[31] X.L. Wu, G.G. Siu, C.L. Fu, H.C. Ong, Photoluminescence and cathodoluminescence studies of stoichiometric and oxygen-deficient ZnO films, Applied Physics Letters 78 (2001) 2285.
[32] H.S. Kang, J.S. Kang, J.W. Kim, S.Y. Lee, Annealing effect on the property of ultraviolet and green emissions of ZnO thin films, Journal of Applied Physics 95 (2004) 1246.
[33] H.S. Kang, J.S. Kang, S.S. Pang, E.S. Shim, S.Y. Lee, Variation of light emitting properties of ZnO thin films depending on post-annealing temperature, Materials Science and Engineering: B 102 (2003) 313.